

A Light-weight Interpretable Compositional Network for Nuclei Detection and Weakly-supervised Segmentation

Yixiao Zhang¹, Adam Kortylewski¹, Qing Liu¹, Seyoun Park¹, Benjamin Green¹, Elizabeth Engle¹, Guillermo Almodovar¹, Ryan Walk¹, Sigfredo Soto-Diaz¹, Janis Taube¹, Alex Szalay¹, and Alan Yuille¹

Johns Hopkins University, Baltimore MD 21218, USA

Abstract. The field of computational pathology has witnessed great advancements since deep neural networks have been widely applied. These deep neural networks usually require large numbers of annotated data to train vast parameters. However, it takes significant effort to annotate a large histopathology dataset. We propose to build a data-efficient model, which only requires partial annotation, specifically on isolated nucleus, rather than on the whole slide image. It exploits shallow features as its backbone and is light-weight, therefore a small number of data is sufficient for training. What’s more, it is a generative compositional model, which enjoys interpretability in its prediction. The proposed method could be an alternative solution for the data-hungry problem of deep learning methods.

Keywords: Compositional Networks · Nuclei detection and segmentation · Generative modeling

1 Introduction

Histopathology images provide an understanding of the microenvironment of various diseases. nucleus detection and segmentation is an important step for the quantitative analysis of cell distributions. Even though hematoxylin and eosin (H&E) stain is the most widely used stain and often the gold standard to visualize the cell structures of histological section, there have been efforts to develop different types of stains and image modalities. Especially, multiplexed immunofluorescence (mIF) and immunohistochemistry (IHC) are emerging technologies with better predictions [13] for immunotherapy.

Deep convolutional neural networks (DNNs) have shown remarkable and reliable performance in various medical image detection and segmentation including histopathology images [23,28,6,14,11,4]. However, the collection of a large number of annotated data is critical and becomes a bottleneck to train conventional DNNs for the analysis of new modalities [12,15]. For example, in an in-house mIF dataset, there are on average 3053 nuclei on an image of size 1404×1872 , which far exceeds the typical number of objects in natural images. It takes dozens of

hours for a trained annotator to label the foreground mask for all nuclei on a field image. In addition, touching nuclei add difficulty to the annotation work, as sometimes it is difficult even for experts to distinguish between a single large nucleus and two small ones tightly cohere to together.

Another insufficiency of current deep learning workflow is that most works regard DNNs as a black box discriminative model without exploring its intermediate representations, thus having little interpretability in the prediction. Considering cell structures, especially nuclei shapes are invariant by stains, generative models for nucleus detection and segmentation learned from a small dataset are an alternative for efficient and robust analysis of various histopathology images.

Aware of the challenges stated above, we propose a light-weight interpretable model inspired by the CompositionalNets [9] for nucleus detection and weakly supervised segmentation on DAPI (4',6-diamidino-2-phenylindole) stained images. CompositionalNets were shown to be successful on natural images, but little has been studied on their applicability on histopathology images. Our proposed model is a generative model in terms of the neural features of a deep neural network. It is able to locate nuclei by finding image regions that it can explain with high likelihood, while also providing human interpretable explanations of its prediction, due to the explicit part-based modeling of nuclei. To increase the performance of CompositionalNet on distinguishing touching nuclei that are hard to locate and segment precisely, we introduce a near-convex shape decomposition algorithm that splits a foreground segmentation into single nucleus, which also serves as a prior likelihood of nuclei locations for the CompositionalNet.

Two highlight features of the proposed method are that it is data-efficient and light-weight. It only requires image patches of isolated nucleus for training, which is much easier to annotate than the whole slide image. Besides, we empirically found that shallow layers (from first stage of U-Net [19]) are able to serve as backbone for the compositional model, which makes the whole model extremely light-weight. Our experiments demonstrate that by carefully exploiting shallow features and geometric cues, we can achieve comparable performance with deep network counterparts in nucleus detection and weakly-supervised segmentation.

2 Related Work

Nucleus Detection There have been a surge of interest in the application of deep learning to nucleus detection [25,28,8,18,20]. Some works adapts a top-down object detector to histopathology images [3,2], while others employ a PMap representation where values represent the proximity to or probability of a nucleus center [26,21,6]. The prediction of PMap can be formed as either a classification or regression problem. Most of these works use a fairly deep network (>10 layers) and require annotation of all nuclei.

Weakly-supervised Nucleus Segmentation Recently, there have been works that explore nucleus segmentation with weak supervision. [12] generates pseudo-labels and progressively generates full training label with scribble annotation. [15] uses Voronoi algorithm and KMeans clustering to derive coarse labels

from nucleus point annotation. [16] predicts uncertainty by a BayesianCNN then select hard nuclei for mask annotation. These works save labelling effort by using weak annotation, but they still need collection of a large dataset to train deep networks.

3 Methodology

In Section 3.1, we introduce background of CompositionalNets, a neural architecture design that was introduced in [10,9] for image classification of single objects. We discuss our extension to nucleus detection in Section 3.3. Finally, we discuss how prior knowledge about the near-convex shape of nuclei can be integrated into probabilistic compositional models to facilitate the separation of touching nuclei in Section 3.4. The flowchart of the whole method is illustrated in Figure 1.

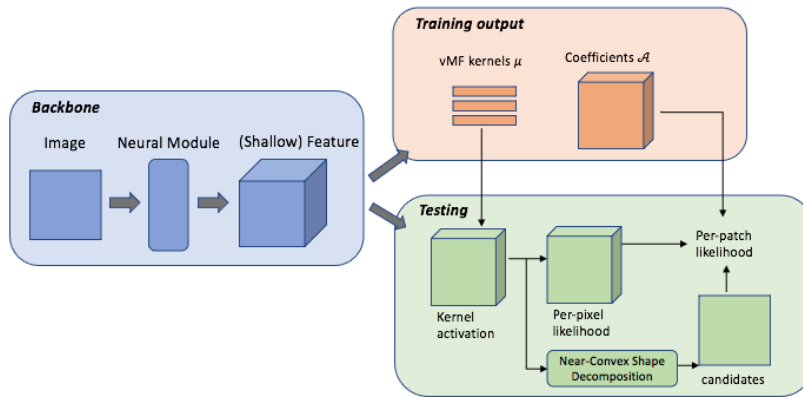


Fig. 1: Flowchart of the proposed method. U-Net stage 1 module was used as the backbone. For training, we cropped nucleus image patches and unsupervisedly learn model parameters (μ and \mathcal{A}). During testing, we apply the model in a sliding window and compute a likelihood for each patch.

3.1 Background on CompositionalNet

CompositionalNet [9] models the generation process of a feature map from a CNN as a mixture of templates. Given a feature map $F \in \mathbb{R}^{H \times W \times D}$, with H and W being the spatial size and D being the channel size. The feature vector f_i at position i are assumed independent and to be modeled as a mixture of

von-Mises-Fisher (vMF) distributions:

$$p(F|\mathcal{A}, \Lambda) = \prod_i p(f_i|\mathcal{A}_i, \Lambda) \quad (1)$$

$$p(f_i|\mathcal{A}_i, \Lambda) = \sum_k \alpha_{i,k} p(f_i|\mu_k), \quad (2)$$

$$p(f_i|\mu_k) \propto \exp\{\sigma f_i^T \mu_k\}, \text{ where } \|f_i\| = 1, \|\mu_k\| = 1 \quad (3)$$

where $\mathcal{A} = \{\alpha_{i,k}\}$ are the mixture coefficients and $\Lambda = \{\mu_k\}$ are kernels for each vMF distribution, which can be regarded as the "mean" feature vector of each mixture component. As in [9], we set the hyperparameter σ in vMF distribution as fixed for tractability. Given a set of feature maps from a pre-trained CNN, the mixture coefficients $\{\alpha_{i,k}\}$ and the vMF kernels $\{\mu_k\}$ can be learned via Maximum Likelihood Estimation.

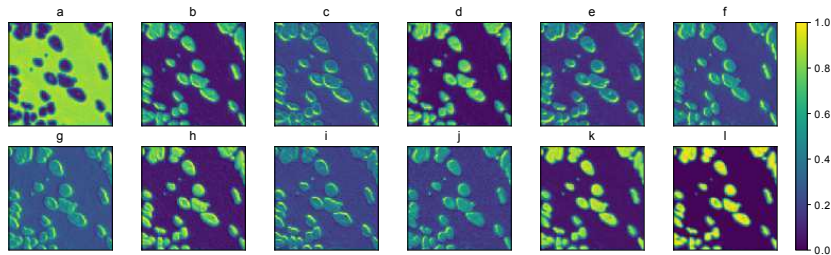


Fig. 2: Activations of vMF kernels on a sample image. (a) is a kernel for background, (b-j) are kernels for various types of edges, and (k-l) are kernels that detect the cell interior texture.

3.2 Interpretable Modeling of Nucleus

The vMF kernels respond to image patterns that frequently occur in the training data. In prior work [10,9] the kernels were shown to correspond to object parts, such as tires of a car. Figure 2 illustrates that we observe a similar property, as the feature vectors that are close to the vMF kernels resemble nucleus parts (background, edges or interior patterns).

An important property of convolutional networks is that the spatial information from the image is preserved in the feature maps. The set of mixture coefficients $\{\alpha_{i,k}\}$ describe the expected activation of a kernel μ_k at a position i , and α_k at all positions can be intuitively thought of as a 2D template, which describes the expected spatial activation pattern of parts in an image of a nucleus - *eg* .where the edges are expected to be located in the image. Therefore,

the decision of the CompositionalNet can be interpreted as first detecting parts, then spatially combining them into a hypothesis about the objects’ presence. Note that this implements a part-based voting mechanism.

As the spatial pattern of parts varies significantly with the shape and size of nuclei, we represent F as a mixture of compositional models:

$$p(F|\Theta) = \sum_m \nu_m p(F|\mathcal{A}^m), \quad (4)$$

with $\mathcal{V}=\{\nu^m \in \{0, 1\}, \sum_m \nu_m=1\}$. Here M is the number of compositional models in the mixture distribution and ν_m is a binary assignment variable that indicates which mixture component is active. Intuitively, each mixture component m will represent a different set of nuclei with specific shape and size (see Figure 3). The parameters of the mixture components $\{\mathcal{A}^m\}$ need to be learned in an EM-type manner by iterating between estimating the assignment variables \mathcal{V} and maximum likelihood estimation of $\{\mathcal{A}^m\}$ [9].

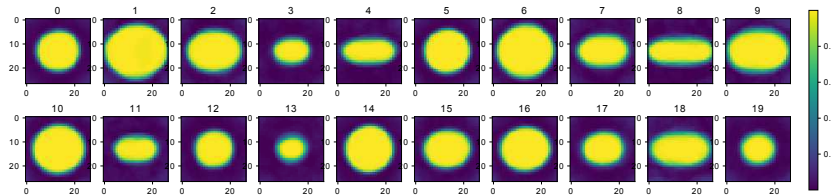


Fig. 3: Average nucleus foreground pattern in each mixture component. Different mixture components are responding to nuclei with different sizes and shapes.

3.3 Adaptation to Nucleus Detection

Previous work has extended CompositionalNet to object detection in natural images [24]. However, it is limited by the assumption that only one salient object is present in an image. Due to the significant difference between histopathology images and natural images, the adaptation for nucleus detection is non-trivial.

First, the background in DAPI stained histopathology images is simpler to model than natural images. However, this encourages the model to rely heavily on the background signals, which is undesirable and results in ambiguity in background regions. We propose to get rid of the negative impact of background signals by masking. For each mixture component m , we pick a subset from \mathcal{A}^m to obtain a soft foreground mask:

$$M^m = \sum_{k \in K_f} \alpha_k^m \quad (5)$$

where K_f is a subset of vMF kernels which represents foreground parts (interior, edge, etc.). Then, we modify the computation of log-likelihood of $p(F|\mathcal{A}^m)$ as:

$$\log p(F|\mathcal{A}^m) = \frac{\sum_i M_i^m \log p(f_i|\mathcal{A}_i^m, A)}{\sum_i M_i^m} \quad (6)$$

which gives more weights to vMF kernels activated at foreground.

Second, we generalize the generative model in compositional networks to multiple objects by extending the model likelihood:

$$p(\mathcal{F}) = \prod_i \prod_n p(F_i)^{z_{i,n}} \quad (7)$$

where F_i are patches from a whole feature map \mathcal{F} , and $\{z_{i,n} \in \{0, 1\} | \sum_n z_{i,n} = 1\}$ are indicators of existence of object n at patch F_i . Note that by the design of the likelihood, only one object model can be active at any location in the feature map. We maximize the likelihood defined in Equation 7 by applying the CompositionalNet in a sliding window manner, and subsequently selecting the local maxima in the response map with non-maximum suppression.

3.4 Deal with touching nuclei

Nuclei usually clump and touch with each other, which makes it difficult to recognize single nucleus. The compositional model is able to explain for a single nucleus, but insufficient to separate touching nuclei precisely. Inspired by [17], we propose to segment nucleus candidates by near-convex shape decomposition. The candidates are integrated into the compositional model as a prior, telling the model where to pay attentions.

First, we select the vMF kernel μ_0 that respond to the background. Given a feature map F , we compute $1 - \mu_0^T f_i$ at each position i to obtain a nucleus foreground score map. A threshold is applied on the score map to give foreground connected components. These connected components may consist of a single nucleus or touching nuclei. To distinguish between them, we leverage the following observations: 1) The shapes of nuclei are usually convex. 2) When multiple nuclei cluster together, there are usually concave points along the boundary of the connected component. Based on these observations, we propose to use a near-convex shape decomposition algorithm to process each connected component.

Following [17], a near-convex decomposition of a shape S , $D_\psi(S)$, is defined as a set of non-overlapping parts:

$$D_\psi(S) = \{P_i | \bigcup_i P_i = S, \forall P_i \cap P_j = \emptyset, c(P_i) \leq \psi\} \quad (8)$$

$$c(P_i) = \max_{v_1, v_2 \in \text{Boundary}(P_i)} \{c(v_1, v_2)\} \quad (9)$$

$$c(v_1, v_2) = \begin{cases} \max_u d(u, v_1 v_2) & \text{if line segment } v_1 v_2 \text{ is outside } P_i \\ 0 & \text{otherwise} \end{cases} \quad (10)$$

where P_i denotes the decomposed parts; ψ is a parameter for near-convex tolerance. Concavity $c(P_i)$ is given by max of concavity $c(v_1, v_2)$ for any two points v_1, v_2 on the boundary of P_i , which is intuitively defined as the max distance from a point u between v_1, v_2 on the boundary to the line segment v_1v_2 .

Besides, a set of potential cuts is needed to split S . We compute the curvature of the boundary of S , and find concave points with negative curvature. A potential cut is formed by the line segment between two concave points if the line segment lies inside S . To comply with the near-convex constraint, all v_1, v_2 with $c(v_1, v_2) > \psi$ must be cut into different parts. These pairs of points are named mutex pairs. Let N be the number of potential cuts and M be the number of mutex pairs. We record two matrices $A_{N \times M}$ and $B_{N \times N}$, where A indicates whether a cut splits a mutex pair, and B indicates whether two cuts intersect with each other:

$$A_{ij} = \begin{cases} 1 & \text{if cut } i \text{ splits mutex pair } j, \\ 0 & \text{otherwise.} \end{cases} \quad B_{ij} = \begin{cases} 1 & \text{if cut } i \text{ intersects with cut } j, \\ 0 & \text{otherwise.} \end{cases}$$

Following [17], the shape decomposition is formed as an integer programming problem:

$$\min w^T x \quad s.t. Ax \geq 1, x^T Bx = 0, x \in \{0, 1\}^N \quad (11)$$

where x is a Boolean selection variable for each potential cut. The first constraint says that every mutex pair should be splitted by some cut, and the second one says that the selected cuts should not intersect with each other. w is a weight vector for each cut defined as: $w_{pq} = \exp\{\langle \vec{n}_p, \vec{p}\vec{q} \rangle\} + \exp\{\langle \vec{n}_q, \vec{q}\vec{p} \rangle\} + \exp\{\lambda \|\vec{p}\vec{q}\|\}$, where p and q are cut endpoints, \vec{n} is the normal vector of the boundary, and $\langle \bullet, \bullet \rangle$ denotes the angle between two vectors. λ is set to 0.1. The selected cuts are encouraged to be perpendicular to the local boundary and be short, which are in accord with human intuition.

Nuclei Candidates as Prior After decomposing the nuclei foreground connected components, the obtained regions are near convex and are taken as candidates of single nucleus. These candidates serve as a prior guiding where to pay attention to for nucleus detection. We define the prior probability of nucleus existence q as Gaussian distributions centered at each candidate. The final detection likelihood score is obtained by integrating the prior into the CompositionalNet such that the final detection map is defined as:

$$p(\mathcal{F}) = \prod_i \prod_n p(F_i)^{z_{i,n}} q(i). \quad (12)$$

3.5 Weakly-supervised Nuclei Segmentation

The nuclei candidates obtained from Section 3.4 can also be used as segmentation masks. Since the algorithm only receives bounding box as supervision which is used to crop nucleus images, it achieves segmentation masks in a weakly-supervised way. The obtained segmentation masks have a property to be near

convex. Although rare nuclei can have concave shapes and be wrongly cut, it can be indicative of potential annotation errors (*eg* .where the annotator mistakenly recognized a pair of touching nuclei as a single one).

4 Experiments

Dataset The mIF images were obtained using Vectra-3 and Vectra Polaris microscopes (Akoya BioSciences, MA, USA) from six patients with liver cancer (3), lung adenocarcinoma (1), lung small cell carcinoma (1), and melanoma (1). The whole slide consists of hundreds of fields in general, and each field has 1872×1404 (*width* \times *height*) size with 32-bit pixel-depth. Total 6 fields, randomly selected from each patient, were used for the experiment in this study. For nucleus detection and segmentation, DAPI stained images were used in this study among the multispectral images. The selected fields were manually checked and annotated by trained researchers and totally 18312 nuclei were annotated. Each field was divided to (256×256) patches which gives totally 210 patches, from which 186 patches were used for training and 24 patches were used for testing.

4.1 nucleus detection

Evaluation metrics. Following [21,8,1,5], we adopt the commonly used precision (P) - recall (R) metrics to evaluate nucleus detection methods. If a predicted nucleus central point is in the proximity of 3 pixels to a ground truth point, it is regarded as true positive, otherwise it is regarded as false positive. If a ground truth point has no corresponding prediction, it is regarded as false negative. By binarizing the predicted score map at different thresholds, we can get a series of precision and recall values and plot them as P-R curve.

Implementation details. The architecture of our CompositionalNet consists of the first two layers of U-Net [19] backbone, followed by a generative compositional model as defined in Section 3. The proposed design leads to a quite light-weight model, which has totally only 213K parameters.

The vMF kernels (Figure 2) are learned in an unsupervised manner by maximum likelihood estimation. We empirically found that 12 kernels are sufficient to model parts of a nucleus. We extracted 2858 isolated nuclei to learn the mixture parameters $\{\mathcal{A}^m\}$. These nuclei were cropped as 27×27 patches, aligned by orientation, and clustered into $M = 20$ clusters using KMeans by their length of long axis and short axis. A compositional model was learned for each cluster of nuclei with specific size and shape (Figure 3). To deal with various orientations of nuclei, we rotated images by $[-90, -60, -30, 30, 60]$ degrees before input, and restore the original rotation after getting output from the model. To improve the performance on touching nuclei, we apply the near-convex decomposition prior as discussed in Section 3.4, where ψ was set to 3 pixels and the variance of the Gaussian distribution was $\sigma = 10$.

Baselines. Recently many advanced deep learning models have achieved state-of-the-art performance on nucleus detection [6]. However, our motivation

is to develop data-efficient models in order to save annotation efforts, at the same time exploit internal representations to make it interpretable. Therefore, We compare our model with two classic baselines: a patch-based CNN [22] and U-Net [19]. The CNN model is designed for nucleus detection and comprises of 2 convolution layers with maxpooling and 3 fully connected layers. We adapted the last spatially constrained layer to a softmax layer to classify an image patch. It was trained with 11K 27x27 image patches of nuclei and the same amount of negative patches with a distance of least 3 pixel to a nucleus center. During testing, the network predicts the probability of being a nucleus center for each pixel. Note that this network has 893K parameters, 3 times more than the proposed model.

The U-Net baseline is an 18-layer network which has 17M parameters. It is trained with full image supervision for 20 epochs by Adam optimizer with learning rate 1e-4 and batch size 8. Following many previous works [26,6,27,5], we implement detection as structured regression to a proximity map. We generated the proximity map by putting a Gaussian distribution function with $\sigma = 2$ at the center of each nucleus, and let the model pixel-wisely regress this proximity map. During inference, local maxima on the regressed map with non-maximum suppression are obtained as detected nucleus centers.

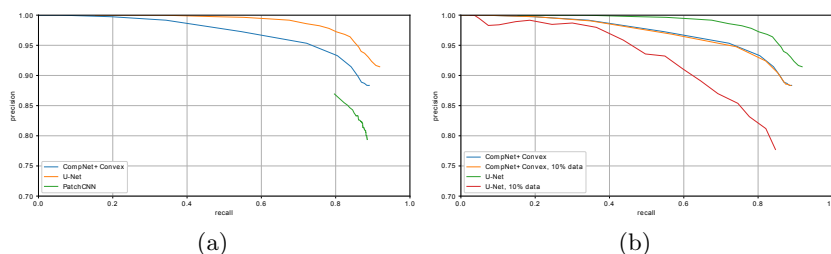


Fig. 4: Evaluation of nucleus detection by Precision-Recall curve. (a) Trained with full data; (b) Trained with 10% data.

| | AJI | DSC |
|--------------------|---------------|---------------|
| BBTP | 0.6765 | 0.8513 |
| WeaklySegPointAnno | 0.5991 | 0.7805 |
| Ours | 0.7030 | 0.8900 |

Table 1: Weakly supervised segmentation results on the proposed dataset.

Results. Figure 4 shows the P-R curve of the baseline CNN, U-Net and the proposed method. The patch-based CNN has exactly the same size of field of view with the proposed model, and is trained with more data (11K nucleus

including both isolated and non-isolated ones). However, our method surpasses it by a large margin, which shows the effectiveness and data efficiency of our method.

Due to extended model complexity and large amount of training data, U-Net outperforms the proposed method when trained with full data. Note that the total number of parameters in the proposed model is 213K, only about 1.2% of the U-Net. What’s more, deep neural networks like U-Net are data hungry and need large amount of data to learn their parameters, while our method only requires annotating the isolated nuclei, which saves much effort for human experts. When data is limited (see Figure 4(b)), the performance of U-Net degrades significantly, while our model is able to maintain the performance. This shows that the proposed method requires less annotated data than deep networks to achieve satisfactory performance.

4.2 Weakly-supervised Nuclei Segmentation

The learning of the proposed method only requires the annotation of nucleus positions and bounding boxes. As stated in Section 3.5, by utilizing the unsupervisedly learned vMF kernels and the near-convex decomposition algorithm, we can obtain nuclei instance segmentation masks. We compare with two weakly-supervised segmentation methods, BBTP [7] and WeaklySegPointAnno [15]. BBTP is a well-known weakly-supervised model for natural images, and WeaklySegPointAnno is developed for nuclei segmentation. Aggregated Jaccard Index (AJI) [11] and Dice similarity coefficient (DSC) were used as metrics:

$$AJI = \frac{\sum_{i=1}^n |G_i \cap S(G_i)|}{\sum_{i=1}^n |G_i \cup S(G_i)| + \sum_{k \in K} |S_k|}, \quad DSC = \frac{2|A \cap B|}{|A| + |B|} \quad (13)$$

where $S(G_i)$ is the segmented object that has maximum overlap with G_i , K is the set of segmented objects that are not assigned to ground-truth objects, and A and B are pixels of ground-truth foreground and segmentation foreground respectively. AJI focuses more on the correct matching between segmented nuclei instances and ground-truths, while DSC focuses on the foreground/background classification.

Table 1 shows the segmentation performance of the methods. The proposed model outperforms BBTP and WeaklySegPointAnno, which verified the effectiveness of our method. What’s more, the proposed model requires little training (only the clustering of vMF kernels), which is an advantage over deep networks. Qualitative results are shown in Figure 5. The proposed method is able to precisely locate the foreground and cut touching nuclei, even for hard cases where more than two nuclei are touching with each other as showed in Figure 5 (a) and (b).

5 Conclusion

We introduced a compositional generative model to the task of nucleus detection and segmentation for DAPI stained histopathology images. It has the following

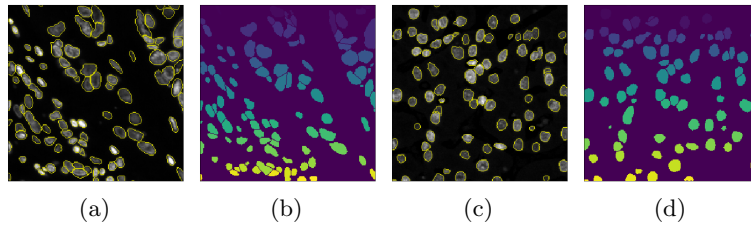


Fig. 5: Qualitative segmentation results. (a) and (c) are DAPI images with nucleus boundary annotated. (b) and (d) are corresponding segmentation results.

merits: data-efficient, light-weight and interpretable. We also proved that by exploiting shallow features from a neural network we can achieve satisfactory performance on the task of nucleus detection and segmentation. For future study, we expect that the proposed method can be combined with transfer learning, where features pre-trained on one histopathology dataset can be exploited to build compositional models on another dataset with different stains.

References

1. Alom, M.Z., Yakopcic, C., Taha, T.M., Asari, V.K.: Microscopic nuclei classification, segmentation and detection with improved Deep Convolutional Neural Network (DCNN) approaches (2018)
2. Baykal, E., Dogan, H., Ercin, M.E., Ersoz, S., Ekinici, M.: Modern convolutional object detectors for nuclei detection on pleural effusion cytology images. *Multimedia Tools and Applications* **79**(21-22) (2020). <https://doi.org/10.1007/s11042-019-7461-3>
3. Du, J., Li, X., Li, Q.: Detection and Classification of Cervical Exfoliated Cells Based on Faster R-CNN. In: 2019 IEEE 11th International Conference on Advanced Infocomm Technology, ICAIT 2019 (2019). <https://doi.org/10.1109/ICAIT.2019.8935931>
4. Graham, S., Vu, Q.D., Raza, S.E., Azam, A., Tsang, Y.W., Kwak, J.T., Rajpoot, N.: Hover-Net: Simultaneous segmentation and classification of nuclei in multi-tissue histology images. *Medical Image Analysis* **58** (2019)
5. Hagos, Y.B., Narayanan, P.L., Akarca, A.U., Marafioti, T., Yuan, Y.: ConCORDe-net: Cell count regularized convolutional neural network for cell detection in multiplex immunohistochemistry images. In: *Lecture Notes in Computer Science (including subseries Lecture Notes in Artificial Intelligence and Lecture Notes in Bioinformatics)*. vol. 11764 LNCS (2019)
6. Höfener, H., Homeyer, A., Weiss, N., Molin, J., Lundström, C.F., Hahn, H.K.: Deep learning nuclei detection: A simple approach can deliver state-of-the-art results. *Computerized Medical Imaging and Graphics* **70** (2018), <https://www.sciencedirect.com/science/article/pii/S0895611118300806>
7. Hsu, C.C., Hsu, K.J., Tsai, C.C., Lin, Y.Y., Chuang, Y.Y.: Weakly supervised instance segmentation using the bounding box tightness prior. In: *Advances in Neural Information Processing Systems*. vol. 32 (2019)

8. Kashif, M.N., Raza, S.E., Sirinukunwattana, K., Arif, M., Rajpoot, N.: Hand-crafted features with convolutional neural networks for detection of tumor cells in histology images. In: Proceedings - International Symposium on Biomedical Imaging. vol. 2016-June (2016)
9. Kortylewski, A., Liu, Q., Wang, A., Sun, Y., Yuille, A.: Compositional Convolutional Neural Networks: A Robust and Interpretable Model for Object Recognition Under Occlusion (2020)
10. Kortylewski, A., Liu, Q., Wang, A., Sun, Y., Yuille, A.: Compositional convolutional neural networks: A robust and interpretable model for object recognition under occlusion. pp. 1–25. Springer (2020)
11. Kumar, N., Verma, R., Sharma, S., Bhargava, S., Vahadane, A., Sethi, A.: A Dataset and a Technique for Generalized Nuclear Segmentation for Computational Pathology. *IEEE Transactions on Medical Imaging* **36**(7) (2017)
12. Lee, H., Jeong, W.K.: Scribble2label: Scribble-supervised cell segmentation via self-generating pseudo-labels with consistency. In: Lecture Notes in Computer Science (including subseries Lecture Notes in Artificial Intelligence and Lecture Notes in Bioinformatics). vol. 12261 LNCS (2020)
13. Lu, S., Stein, J.E., Rimm, D.L., Wang, D.W., Bell, J.M., Johnson, D.B., Sosman, J.A., Schalper, K.A., Anders, R.A., Wang, H., Hoyt, C., Pardoll, D.M., Danilova, L., Taube, J.M.: Comparison of Biomarker Modalities for Predicting Response to PD-1/PD-L1 Checkpoint Blockade: A Systematic Review and Meta-analysis. *JAMA Oncology* **5**(8), 1195–1204 (2019)
14. Naylor, P., Lae, M., Reyat, F., Walter, T.: Nuclei segmentation in histopathology images using deep neural networks. In: Proceedings - International Symposium on Biomedical Imaging (2017)
15. Qu, H., Wu, P., Huang, Q., Yi, J., Yan, Z., Li, K., Riedlinger, G.M., De, S., Zhang, S., Metaxas, D.N.: Weakly Supervised Deep Nuclei Segmentation Using Partial Points Annotation in Histopathology Images. *IEEE transactions on medical imaging* **39**(11) (2020)
16. Qu, H., Yi, J., Huang, Q., Wu, P., Metaxas, D.: Nuclei Segmentation Using Mixed Points and Masks Selected from Uncertainty. In: Proceedings - International Symposium on Biomedical Imaging. vol. 2020-April (2020)
17. Ren, Z., Yuan, J., Li, C., Liu, W.: Minimum near-convex decomposition for robust shape representation. In: Proceedings of the IEEE International Conference on Computer Vision (2011)
18. Rojas-Moraleda, R., Xiong, W., Halama, N., Breikopf-Heinlein, K., Dooley, S., Salinas, L., Heermann, D.W., Valous, N.A.: Robust detection and segmentation of cell nuclei in biomedical images based on a computational topology framework. *Medical Image Analysis* **38** (2017)
19. Ronneberger, O., Fischer, P., Brox, T.: U-net: Convolutional networks for biomedical image segmentation. In: Lecture Notes in Computer Science (including subseries Lecture Notes in Artificial Intelligence and Lecture Notes in Bioinformatics). vol. 9351 (2015)
20. Schmidt, U., Weigert, M., Broaddus, C., Myers, G.: Cell detection with star-convex polygons. In: Lecture Notes in Computer Science (including subseries Lecture Notes in Artificial Intelligence and Lecture Notes in Bioinformatics). vol. 11071 LNCS (2018). https://doi.org/http://dx.doi.org/10.1007/978-3-030-00934-2_30, <https://link.springer.com/chapter>
21. Sirinukunwattana, K., Ahmed Raza, S.E., Tsang, Y.W., Snead, D., Cree, I., Rajpoot, N.: A spatially constrained deep learning framework for detection of epithelial tumor nuclei in cancer histology images. In: Lecture Notes in Computer Science

- (including subseries Lecture Notes in Artificial Intelligence and Lecture Notes in Bioinformatics). vol. 9467 (2015)
22. Sirinukunwattana, K., Raza, S.E., Tsang, Y.W., Snead, D.R., Cree, I.A., Rajpoot, N.M.: Locality Sensitive Deep Learning for Detection and Classification of Nuclei in Routine Colon Cancer Histology Images. *IEEE Transactions on Medical Imaging* **35**(5) (2016)
 23. Tofighi, M., Guo, T., Vanamala, J.K., Monga, V.: Deep networks with shape priors for nucleus detection. In: *Proceedings - International Conference on Image Processing, ICIP* (2018)
 24. Wang, A., Sun, Y., Kortylewski, A., Yuille, A.: Robust object detection under occlusion with context-aware compositionalnets. In: *Proceedings of the IEEE Computer Society Conference on Computer Vision and Pattern Recognition* (2020)
 25. Wang, S., Yao, J., Xu, Z., Huang, J.: Cell detection with an accelerated deep convolution neural network. In: *Lecture Notes in Computer Science (including subseries Lecture Notes in Artificial Intelligence and Lecture Notes in Bioinformatics)*. vol. 9901 LNCS (2016)
 26. Xie, Y., Xing, F., Kong, X., Su, H., Yang, L.: Beyond classification: Structured regression for robust cell detection using convolutional neural network. In: *Lecture Notes in Computer Science (including subseries Lecture Notes in Artificial Intelligence and Lecture Notes in Bioinformatics)*. vol. 9351 (2015)
 27. Xie, Y., Xing, F., Shi, X., Kong, X., Su, H., Yang, L.: Efficient and robust cell detection: A structured regression approach. *Medical Image Analysis* **44** (2018)
 28. Xu, J., Xiang, L., Liu, Q., Gilmore, H., Wu, J., Tang, J., Madabhushi, A.: Stacked sparse autoencoder (SSAE) for nuclei detection on breast cancer histopathology images. *IEEE Transactions on Medical Imaging* **35**(1) (2016)